Master's Thesis

석사 학위 논문

Dual regulation of R-type $Ca_V2.3$ current by G_q-coupled receptors

Jin-Young Jeong (정진영 **鄭 珍 英**)

Department of Brain and Cognitive Sciences

뇌 · 인지과학전공

DGIST

2015

Dual regulation of R-type $Ca_V2.3$ current by G_q-coupled receptors

Advisor : Professor Byung-Chang Suh
Co-advisor : Professor Ho-Jeong Kim

by

Jin-Young Jeong
Department of Brain and Cognitive Sciences
DGIST

A thesis submitted to the faculty of DGIST in partial fulfillment of the requirements for the degree of Master of Science in the Department of Brain and Cognitive Sciences. The study was conducted in accordance with Code of Research Ethics[1)].

06. 03. 2015

Approved by

Professor Byung-Chang Suh (Signature)
(Advisor)

Professor Ho-Jeong Kim (Signature)
(Co-Advisor)

1) Declaration of Ethical Conduct in Research**:** I, as a graduate student of DGIST, hereby declare that I have not committed any acts that may damage the credibility of my research. These include, but are not limited to: falsification, thesis written by someone else, distortion of research findings or plagiarism. I affirm that my thesis contains honest conclusions based on my own careful research under the guidance of my thesis advisor.

Dual regulation of R-type $Ca_V2.3$ current by G_q-coupled receptors

Jin-Young Jeong

Accepted in partial fulfillment of the requirements for the degree of
Master of Science

06. 03. 2015

Head of Committee _____ (Signature)

Prof. Byung-Chang Suh

Committee Member _____ (Signature)

Prof. Ho-Jeong Kim

Committee Member _____ (Signature)

Prof. Kyuhyung Kim

MS/BS

201325012

정진영, Jin-Young Jeong, Dual regulation of R-type $Ca_V2.3$ current by G_q-coupled receptors

Department of Brain and Cognitive Sciences. 2015. 69p.

Professor Byung-Chang Suh, Professor Ho-Jeong Kim

Abstract

Many high voltage-activated Ca^{2+} channels are modulated by G_q-coupled M_1 muscarinic acetylcholine receptors. $Ca_V2.3$ currents are known to be increased by M_1 receptor activation, and the increase in the $Ca_V2.3$ currents is mediated by phosphorylation of $Ca_V2.3$ channel via the activation of protein kinase C (PKC). Here, we report that M_1 muscarinic receptors can also inhibit $Ca_V2.3$ currents when the channels are fully activated by PKC. In the whole-cell configuration of tsA201 cells, phorbol 12-myristate 13-acetate (PMA), a PKC activator, potentiated $Ca_V2.3$ currents by ~ 2-fold. We found that after the PMA-induced potentiation of $Ca_V2.3$ currents, application of the M_1 receptor agonist oxotremorine-M (Oxo-M), decreased the currents by 52%. We examined if the hydrolysis of plasma membrane phosphoinositides (PIs) were involved in the muscarinic suppression of $Ca_V2.3$ currents. We used two methods to deplete $PI(4,5)P_2$; voltage-sensing phosphatase (VSP), and rapamycin-induced translocatable pseudojanin (PJ) system. Activation of VSP suppressed $Ca_V2.3$ current by 38%. PJ system could directly dephosphorylate 4- and 5-phosphates from both PI(4)P and $PI(4,5)P_2$ the plasma membrane. After the addition of rapamycin $Ca_V2.3$ currents were dramatically and irreversibly decreased by 66% compared to the initial level. Taken together, our results suggest that $Ca_V2.3$ currents are modulated by M_1 receptor in a dual mode; potentiation by PKC activation and suppression by poly-PI depletion. Activation of M_1 receptors can solely decrease $Ca_V2.3$ currents in the PKC-activated cells. PJ-induced inhibition of $Ca_V2.3$ currents demonstrates that poly-PIs are important in the maintenance of $Ca_V2.3$ channel activity.

Keywords: $Ca_V2.3$ channel, M_1 muscarinic receptor, phosphatidylinositol 4,5-bisphosphate ($PI(4,5)P_2$)

Table of contents

List of figures

1. Introduction

As a signaling molecule, Ca^{2+} ions mediate various physiological events; exocytosis, muscle contraction, metabolism, gene transcription, fertilization, proliferation (1). Ca^{2+} signaling is triggered by transient increase in intracellular Ca^{2+} concentration. Cytosolic Ca^{2+} concentration is low when cell is resting state (approximately 100 nM). However, when an appropriate stimulus arrives, cytosolic Ca^{2+} concentration is suddenly elevated up to 500 nM or more, which is responsible for a change in cellular activities (Figure 1). Voltage-gated calcium channels (VGCCs) deliver extracellular Ca^{2+} ions into cytosol along concentration gradient, and the accumulation of these ions begins a lot of calcium signaling (2). Therefore calcium channels are key transducers of membrane potential changes into intracellular Ca^{2+} transients.

VGCCs are expressed in excitable cells. They induce Ca^{2+} influx in response to membrane potential changes. There are ten VGCCs (Figure 2A). They are classified into two groups depending on its depolarization voltage: high-voltage activated (HVA) and low-voltage activated (LVA) calcium channels. HVA calcium channels have an activation threshold at membrane voltage positive to -20 mV while LVA calcium channels are activated at a membrane voltage positive to -70 mV. In addition, HVA calcium channels are also divided into two groups by sequence homology of α1 subunit. One is L-type channels ($Ca_V1.1$, $Ca_V1.2$, $Ca_V1.3$, and $Ca_V1.4$). The other is neuronal type channels ($Ca_V2.1$, $Ca_V2.2$, and $Ca_V2.3$). LVA channels are T-type channels ($Ca_V3.1$, $Ca_V3.2$, and $Ca_V3.3$). VGCCs are composed of four subunits: α1, β, α2δ, and γ (Figure 2B). α1 subunit forms the voltage-sensitive, Ca^{2+}-selective pore. This subunit has four homologous domains and each domain has six transmembrane segments (Figure 2C). N-terminus, loop connecting domains, and C-terminus have binding sites with molecules such as Gβγ subunits and calmodulin. β, α2δ, and γ subunits are auxiliary subunits. These subunits are able to alter the biophysical properties of the channel, voltage-dependences, rates of activation-inactivation, and increase the trafficking of alpha 1 subunit to the plasma membrane (3-4).

$Ca_V2.3$ channels are distributed to the central nervous system specifically localized to presynaptic

terminal. Their major role is neurotransmitter release. When action potential is delivered to axon terminal, $Ca_V2.3$ channel is opened and calcium influx through this channels triggers neurotransmitter release. $Ca_V2.3$ channels are widely expressed in the brain such as hippocampus, amygdala, olfactory bulb, and frontal cortex (5-7). In addition they are also expressed in dorsal root ganglia (DRG) and sensory neuron. Hence, α1E-/- mice showed abnormal pain response and enhanced fear (8-10).

Even though α1 subunits of Ca_V2 family have high sequence homology, $Ca_V2.3$ channels have different kinetic properties and pharmacological characteristics from $Ca_V2.1$ and $Ca_V2.2$ channels. $Ca_V2.3$ channels are activated at a lower voltage than other Ca_V2 channels. Besides, activation and inactivation of $Ca_V2.3$ channels are faster than $Ca_V2.2$ channels. In a pharmacological aspect, $Ca_V2.3$ channels are insensitive to $Ca_V2.1$ and $Ca_V2.2$ channel blockers such as ω-agatoxin-IVA or ω-conotoxin GVIA (6-7).

G protein-coupled receptors (GPCRs) are known as modulator of VGCC. Two modulatory pathways are involved in this regulation; the “fast” pathway and the “slow” pathway. The “fast” pathway is mediated by heterotirmeric $G_{i/o}$ protein coupled receptor, for example type 2 muscarinic receptor (M_2R). Gβγ subunit dissociated from receptor suppresses Ca_V2-type VGCCs by binding to calcium channel α1 subunit directly. The “slow” pathway is mediated by $G_{q/11}$ protein coupled receptor, for instance type 1 muscarinic receptors (M_1R) (Figure 3). In this pathway, when receptor is activated by its agonist, $G\alpha_q$ subunit activates phospholipase Cβ (PLCβ) embedded in plasma membrane. In turn, PLCβ hydrolyzes plasma membrane $PI(4,5)P_2$ to diacylglycerol (DAG) and inositol 1,4,5-triphosphate (IP_3). DAG recruits and activates cytosolic protein kinase C (PKC) and PKC phosphorylates its target proteins, for example ion channels, transcription factors, and scaffold proteins. IP_3 is translocated to cytosol and binds to IP_3 receptor in endoplasmic reticulum (ER). Ca^{2+} ions stored in ER are released to cytosol (11-12).

As mentioned before, despite high sequence homology of α1 subunits between Ca_V2-type VGCC, $Ca_V2.3$ channels differ from $Ca_V2.1$ and $Ca_V2.2$. The significant difference between $Ca_V2.3$ channel and the other Ca_V2 channels is the modulatory effects of M_1 muscarinic receptor (M_1R) activation. As a G_q protein-coupled receptor, M_1R activation results in hydrolyzation of plasma membrane

phosphatidylinositol 4,5-bisphosphate ($PI(4,5)P_2$). According to the previous studies, $Ca_V2.3$ channels were potentiated by M_1R activation. The enhancement of $Ca_V2.3$ currents occurred through the activation of Ca^{2+}-independent protein kinase C (PKC) by M_1R activation (13-15). On the other hand, $Ca_V2.1$ and $Ca_V2.2$ currents were suppressed by M_1R activation. This suppression was turned out due to Gβγ and $PI(4,5)P_2$ depletion (16-21).

At first, $PI(4,5)P_2$ was paid attention as a substrate of PLC. Now, many studies said $PI(4,5)P_2$ is regulator of ion channels and transporters. There are several regulatory mechanisms. Firstly, $PI(4,5)P_2$ directly binds to ion channels and stabilizes them in a certain state. For instant, $PI(4,5)P_2$ stabilizes the transient receptor potential V1 (TRPV1) in the closed state (22). Secondly, $PI(4,5)P_2$ induces membrane insertion or endocytosis of ion channel (23-24). These mechanisms are mediated by many proteins involved in exocytosis and endocytosis, respectively. Lastly $PI(4,5)P_2$ regulates ion channel through the cytoskeleton (25).

To investigate whether $PI(4,5)P_2$ depletion also affect $Ca_V2.3$ channel modulation, we tested the $PI(4,5)P_2$ sensitivity of $Ca_V2.3$ channels. $PI(4,5)P_2$ depletion by M_1R activation generates several secondary molecules. Hence, we employed voltage-sensitive phosphatase from zebrafish (Dr-VSP) and chemically-induced dimerization (CID) system to selectively dephosphorylate $PI(4,5)P_2$ in plasma membrane. By using these methods, we observed that $Ca_V2.3$ channels were also regulated by membrane $PI(4,5)P_2$. In addition, we tested sensitivities of $Ca_V2.3$ channels to phosphatidylinositol 4-phosphate (PI(4)P), another plasma membrane phosphoinositides. As a result, we suggest that PI(4)P in the plasma membrane is indirectly involved in suppression of $Ca_V2.3$ channels.

2. Materials and methods

2.1 Materials

The following cDNAs were gifted to us: rat α1E (accession number NM_019294) from Terrance P. Snutch, University of British Columbia; rat α1B (accession number NM_001195199), β3 (accession number NM_012828), and α2δ1 (accession number NM_012919) from Diane Lipscombe, Brown University, Providence, RI; rat M_1-muscarinic receptor (accession number NM_080773) from Neil N. Nathanson, University of Washington, WA; Dr-VSP with EGFP from Yasushi Okamura, Osaka University, Osaka, Japan; Lyn_{11}-FRB, PJ-Dead, PJ-Sac, INPP5E, PJ, and PH-PLCδ-GFP from Bertil Hille, University of Washington School of Medicine, Seattle, Washington.

2.2 Cell culture

tsA201 cells (human embryonic kidney cells) were maintained in Dulbecco Modified Eagle Medium (DMEM; Invitrogen) supplemented with 10% Fetal Bovine Serum (FBS; Invitrogen) and 0.2% penicillin/streptomycin (Invitrogen) in 100 π culture dishes (Falcon). Cells were grown at 37 ℃ in a CO_2 (5%) incubator. Passage was performed every 3 to 4 days to a new dish as cell density reached 70%. To detach the cells from culture dish, 1 ml of Ca^{2+}-free Dulbecco's Phosphate-Buffered Saline (DPBS; Life Technologies) was treated and cells were incubated at 37 ℃ for 1 min 30 s. Detached cells were transferred to 15 ml conical tube (Falcon) and centrifuged at 1000 rpm for 1 min 30 s. Pellet was resuspended using 1 ml culture media and moved to new culture dish as cell density reached 20%.

2.3 Transfection

In all experiments, for calcium channel expression the α1B or α1E of Ca_V, β3, and α2δ1 subunits were transiently transfected into tsA201 cells in a 1:1:1 ratio. In some cases 1000 ng M_1 muscarinic receptor (M_1R) or 1000 ng Dr-VSP was co-transfected. For the rapamycin-inducible dimerization experiment 200 ng Lyn_{11}-FRB and 300 ng translocatable enzymes (PJ-Dead, PJ-Sac, INPP5E, and PJ) were co-transfected. Also, for the confocal experiment, 200 ng PH-PLCδ-GFP were co-transfected. The tsA201 cells were allowed to grow on 35 π culture dish and transfection was performed when the confluency of cells reached 60-70%. 10 μl of Lipofectamine 2000 (Invitrogen, CA) was added to 250 μl DMEM and wait for 5 min. cDNA were applied with another 250 μl DMEM. Both solutions were mixed and incubated for 15 min in dark space then the transfectant mixture was added to cells. After 4 h, fresh culture media containing FBS and antibiotics exchanged. Transfected cells were plated onto to the poly-L-lysine (0.1 mg/ml, Sigma-Aldrich, MO) coated chip 48 h later for electrophysiological experiment and 24 h later for the confocal experiment after transfection.

2.4 Solution

The bath solution used to record Ba^{2+} currents contained (in mM): 10 $BaCl_2$, 150 NaCl, 1 $MgCl_2$, 10 HEPES, and 8 glucose (adjusted to pH 7.4 with NaOH). The pipette solution contained (in mM): 175 $CsCl_2$, 5 $MgCl_2$, 5 HEPES, 0.1 1,2-bis(2-aminophenocy)ethane N,N,N',N'-tetraacetic acid (BAPTA), 3 Na_2ATP, and 0.1 Na_3GTP (adjusted to pH7,4 with CsOH). The external solution for confocal imaging contained (in mM): 160 NaCl, 2.5 KCl, 2 $CaCl_2 \cdot H_2O$, 1 $MgCl_2$, 10 HEPES, and 8 glucose (adjusted to pH7.4 with NaOH). The bath solutions were stored in 4 ℃ refrigerator. The pipette solution was stored in the -20 ℃ freezer. The following reagents were obtained: BAPTA, Na_2ATP, Na_3GTP, CsOH, $BaCl_2$ were obtained (Sigma-Aldrich, MO), HEPES (Calbiochem, CA), and other chemicals (Merck, Germany).

2.5 Chemicals

Oxotremorine-M (Oxo-M, Sigma-Aldrich, MO) was dissolved in H_2O to make 10 mM stock. Both phorbol 12-myristate 13-acetate (PMA, Enzo life sciences, NY) and rapamycin (LC Laboratories, MA) were dissolved in dimethyl sulfoxide (DMSO, Sigma-Aldrich, MO) to make 100 μM and 5 mM stock, respectively. All chemicals were stored at -20 ℃ freezer. They were diluted with the bath solution before applied to cells.

2.6 Current recording

All currents were obtained at room temperature (22-25 ℃). Patch pipettes (1-4 MΩ) were pulled from borosilicate glass micropipette capillaries (1.5 mm outer diameter; 1.10 mm inner diameter; and 10 cm length) (Sutter Instrument). The whole-cell configuration was used to record Ba^{2+} currents. In cell attached mode, gigaohm seal was formed, and plasma membrane was ruptured by negative pressure. Series resistance was 3.6-6 MΩ and was compensated by 60%. HEKA EPC-10 amplifier with pulse software (HEKA Elektronik) was used for currents recording. Ba^{2+} currents were recorded with a membrane holding potential of -80 mV and 100-ms test pulse (+10 mV for $Ca_V2.2$ channels and 0 mV for $Ca_V2.3$ channels) was applied every 4 s. For Dr-VSP experiments, following protocol was used. First, test pulse a (+ 10 mV for $Ca_V2.2$ channels and 0 mV for $Ca_V2.3$ channels) was applied for 10 ms. This current became the baseline. Then +120 mV was generated for 1 s to activate Dr-VSP and to deplete $PI(4,5)P_2$. Following the large depolarizing pulse, -150 mV hyperpolarizing pulse was applied for 400 ms to remove calcium channel inactivation. At last, test pulse b was applied. Current a and b, before and after $PI(4,5)P_2$ depletion by Dr-VSP activation, was compared to calculate the ratio of currents inhibition.

2.7 Confocal imaging

Confocal images were obtained with the Carl Zeiss Inverted LSM 700 confocal microscope (Carl

Zeiss AG, GFP by argon-ion laser and mRFP by blue diode laser) at room temperature (22-25 ℃). In time course, images were obtained by scanning cells with a 40X (water) objective lens at 512X512 pixels, and were taken every 10 s, for 5 min. For the single image, cells were scanned with a 40X (water) objective lens at 1024X1024 pixels, and were transferred to JPEG format. Cytosolic fluorescence intensity was measured by using ZEN2010 and was processed with Microsoft Office Excel 2010 (Microsoft) and Igor Pro (WaveMetrics, Inc.).

2.8 Data analysis

For data acquisition and analysis, HEKA EPC-10 amplifier (HEKA Elektronik) was used. Additional data processing accomplished with Igor Pro (WaveMetrics, Inc.) and Microsoft Office Excel 2010 (Microsoft). The time constants were measured by exponential fit. All quantitative data were expressed as the mean ± SEM. Student's *t*-test was used for comparisons between two groups. One-way ANOVA was used for comparisons among more than two groups.

3. Result

To record calcium channel currents, we expressed α1B for $Ca_V2.2$ currents or α1E for $Ca_V2.3$ currents. As auxiliary subunits, β3 having the highest sensitivity to $PI(4,5)P_2$ and α2δ1 were co-transfected. Whole-cell currents were recorded with barium. We used Ba^{2+} as charge carrier instead of Ca^{2+} to rule out calcium-dependent inactivation (CDI) (26) and other unexpected events triggered by Ca^{2+} ions. In all experiments, we used $Ca_V2.2$ channels as a control because they are the well noted to be inhibited by M_1R activation. Peak voltages, + 10 mV for $Ca_V2.2$ and 0 mV for $Ca_V2.3$ channel, were applied to generate Ba^{2+} currents.

3.1 $Ca_V2.3$ currents are suppressed as well as stimulated by M_1 muscarinic receptor

Most high voltage-activated (HVA) calcium channels are known to be inhibited by M_1R activation, but $Ca_V2.3$ channels are activated by M_1R activation (13, 27). TsA201 cells were co-transfected with M_1R and either $Ca_V2.2$ or $Ca_V2.3$ channels. Test pulse was generated every 4 s for 100 ms, and each current was recorded. The external solution containing 10 μM of Oxotremorine-M (Oxo-M), muscarinic receptor agonist, was perfused for 60 s. $Ca_V2.2$ (N-type) currents were rapidly decreased in response to Oxo-M by 55 ± 2% (n=13, Figure 4A and 4C). In contrast, $Ca_V2.3$ (R-type) currents were increased by 83 ± 7% (n=9, Figure 4B and 4C). These results were consistent with previous studies (13, 20, 27-28).

According to the previous studies, phosphorylation of Ca_Vα1 subunits, by protein kinase C (PKC) activates $Ca_V2.3$ channels (29-33). Based on these studies, we decided to verify the effect of PKC on both $Ca_V2.2$ and $Ca_V2.3$ currents. The bath solution containing 1 μM Phorbol 12-myristate 13-acetate (PMA) which is a DAG analogous recruiting PKC to plasma membrane was perfused for 120 s. Then Oxo-M was co-applied with PMA for 60 s in M_1R-expressing cells. While $Ca_V2.2$ currents were not significantly changed by PMA application, $Ca_V2.3$ currents were increased almost 2-fold (Figure 5A

and 5B). Interestingly we found that after full-activation of $Ca_V2.3$ channels by PKC activation, $Ca_V2.3$ currents were decreased by 52 ± 8% (n=5) as like $Ca_V2.2$ currents (47 ± 5% n=9) (Figure 5C). Time constants for Oxo-M-induced inhibition of $Ca_V2.2$ currents and $Ca_V2.3$ currents were 4 ± 0.3 s (n=9) and 12 ± 2 s (n=5), respectively (Figure 5D). Collectively, our results showed that $Ca_V2.3$ channels were also inhibited by M_1R activation like $Ca_V2.2$ channels after full-activation of PKC.

3.2 $Ca_V2.3$ currents are decreased by Dr-VSP activation

Muscarinic inhibition of VGCCs is known to be due to $PI(4,5)P_2$ depletion by PLCβ, so we decided to test the effect of $PI(4,5)P_2$ depletion on $Ca_V2.3$ channels. Dr-VSP was used to transiently dephosphorylate $PI(4,5)P_2$ in plasma membrane and to prevent generation of the secondary signaling molecules by M_1R activation. The protocols used for activating Dr-VSP were represented in Figure 6A. In tsA201 cells expressing both $Ca_V2.2$ channels and Dr-VSP, $Ca_V2.2$ currents were decreased by 40 ± 4% (n=9) after 1 s of depolarizing pulse. In contrast, there was no significant change in the control (-Dr-VSP) cells (Figure 6B left and 6C). Similarly, $Ca_V2.3$ channels were inhibited by Dr-VSP activation like $Ca_V2.2$ channels. The $Ca_V2.3$ currents in cells expressing Dr-VSP were decreased by 38 ± 1% (n=6) in response to $PI(4,5)P_2$ depletion while the control cells were not (Figure 6B right and 6D). These results suggest that the depletion of $PI(4,5)P_2$ by Dr-VSP activation inhibited both $Ca_V2.2$ and $Ca_V2.3$ channels.

3.3 $Ca_V2.3$ currents are decreased by chemically-induced phosphoinositide depletion

To further examine the regulation of $Ca_V2.3$ currents by phosphoinositides, we employed CID system. By using this method, we can selectively and consistently deplete the level of phosphoinositides in the plasma membrane. Here, we executed recently developed Pseudojanin (PJ) system (34). In this system, the phosphatase is conjugated with FK506 binding protein 12 (FKBP), one of the dimerization protein. Following four constructs were used to dephosphorylate plasma membrane

phosphoinositides: PJ-Dead, PJ-Sac, INPP5E and PJ (Figure 7A). PJ-Sac is 4-phosphatase from *S. cerevisiae* sac1. This enzyme dephosphorylates PI(3)P, PI(4)P, and PI(3,5)P_2 but PI(4,5)P_2 is not its substrate (35). INPP5E, inositol polyphosphate-5-phosphatase E, is 5-phosphatase, and their substrates are PI(4,5)P_2 and PI(3,4,5)P_3 (36). In PJ, both PJ-Sac and INPP5E are active and this translocatable enzyme can dephosphorylate both 4- and 5-phosphate at the same time. Opposite to PJ, PJ-Dead is inactive for both phosphatases. Lyn_{11}, plasma membrane targeting motif (37), is fused with FKBP-rapamycin binding protein (FRB). When rapamycin is added, FKBP and FRB form a ternary complex with rapamycin. Hence, the phosphatase conjugated to FKBP is recruited to plasma membrane and dephosphorylates its substrates (Figure 7B).

To monitor the movement of translocatable enzyme, we performed the confocal experiments. TsA201 cells were co-transfected with both Lyn_{11}-FRB and one of the following four translocatable enzymes tagged with mRFP; PJ-Dead, PJ-Sac, INPP5E, or PJ. We also transfected PH-PLCδ-GFP, PI(4,5)P_2 probe. PH domain of PLCδ binds to PI(4,5)P_2 so we can detect plasma membrane PI(4,5)P_2 in live cell. Cells expressing both PH-PLCδ-GFP (green) and translocatable enzymes (red) were shown in Figure 8A. At first, PH-PLCδ-GFP was localized to plasma membrane while each translocatable enzyme, PJ-Dead (Figure 8B, upper left), PJ-Sac (Figure 8B, upper right), INPP5E (Figure 8B, lower left), and PJ (Figure 8B, lower right), existed in cytosol. After application of 1 μM rapamycin, all of the translocatable enzymes rapidly moved to plasma membrane (42 ± 3% for PJ-Dead, n=4; 43 ± 4% for PJ-Sac, n=9; 49 ± 4% for INPP5E, n=7; 57 ± 3 % for PJ, n=9), and their time constant of decrease in cytosolic intensity was similar (17 ± 4s for PJ-Dead, n=4; 17 ± 1s for PJ-Sac, n=9; 14 ± 1s for INPP5E, n=7; 16 ± 2s for PJ, n=9) (Figure 8C left and 8D left). However, the movement of PH-PLCδ-GFP from plasma membrane to cytosol was different depending on the enzyme co-transfected with. Cytosolic fluorescence intensity of PH-PLCδ-GFP co-transfected with PJ-Dead was almost the same before and after treatment with rapamycin (8 ± 2%, n=4). In cells expressing PJ-Sac, PH-PLCδ-GFP was dissociated from plasma membrane, and its cytosolic intensity was increased by 22 ± 4% (n=9). The increase in cytosolic PH-PLCδ-GFP intensity by INPP5E (45 ± 3%, n=7) and PJ (48 ± 7%, n=9) was greater than that of PJ-Sac (Figure 8C right). When PJ-Sac was transfected, time constant of rapamycin-induced increase in cytosolic PH-PLCδ-GFP intensity was 25 ± 4 s (n=9), while that of

INPP5E and PJ was 17 ± 1 s (n=7) and 15 ± 3 s (n=9), respectively (Figure 8D right). Our results showed that PJ-Sac might be involved in $PI(4,5)P_2$ depletion, but the rate of $PI(4,5)P_2$ dephosphorylation by PJ-Sac was slower than that of INPP5E or PJ.

Now, we measured $Ca_V2.2$ and $Ca_V2.3$ currents when translocatable enzymes moved to plasma membrane and dephosphorylated their substrates. The tsA201 cells were transfected with $Ca_V2.2$ or $Ca_V2.3$, Lyn_{11}-FRB, and one of the following phosphatase: PJ-Dead, PJ-Sac, INPP5E, and PJ. The external solution containing 1 μM of rapamycin was perfused for 60 s. $Ca_V2.2$ currents in cells expressing PJ-Sac were decreased by 39 ± 5% (n=9), and the currents expressing INPP5E were decreased by 37 ± 3% (n=5). When the cells were co-transfected with PJ the currents were inhibited by 56 ± 4% (n=11). The recruitment of PJ-Dead had no significant effects on the currents (Figure 9A and 9B). Currents were not recovered because rapamycin-induced dimerization was irreversible and emzymes consistently dephosphorylated $PI(4,5)P_2$. The inhibition of $Ca_V2.2$ currents by the recruitment of PJ-Sac took more time (29 ± 2 s, n=9) than that of INPP5E (10 ± 1 s, n=5) or PJ (7 ± 4 s, n=11) (Figure 9C).

We also examined the $Ca_V2.3$ channel regulation by the translocation of Pseudojanin constructs. The tendency of decrease in $Ca_V2.3$ current was similar to $Ca_V2.2$ channel. The translocation of PJ-Dead had no significant effect on the $Ca_V2.3$ currents (3 ± 5%, n=3). The recruitment of PJ-Sac decreased the $Ca_V2.3$ currents by 37 ± 4% (n=5) while that of INPP5E decreased the currents by 53 ± 3% (n=6). Lastly, PJ induced the strongest decrease in $Ca_V2.3$ current (66 ± 3%, n=7) (Figure 10A and 10B). Like $Ca_V2.2$ currents, translocation of PJ-Sac took more time (39 ± 3 s, n=5) than that of INPP5E (11 ± 1 s, n=6) or PJ (9 ± 1 s, n=7) for decreasing the $Ca_V2.3$ currents (Figure 10C). These results suggested that $Ca_V2.3$ currents were suppressed by depletion of $PI(4,5)P_2$ in the plasma membrane.

4. Discussion

Even though $PI(4,5)P_2$ is known as a crucial regulator of many other ion channels and transporters (40-42), we have not known whether $PI(4,5)P_2$ in plasma membrane can regulate $Ca_V2.3$ channels. Our results indicate that $Ca_V2.3$ channels are suppressed by plasma membrane $PI(4,5)P_2$ depletion only after they were fully activated by PKC (Figure 5B). $Ca_V2.3$ current inhibition was proved by selective dephosphorylation of $PI(4,5)P_2$ in the plasma membrane by using Dr-VSP (Figure 4) and CID system (Figure 9 and Figure 10).

Actually PKC activation itself is enough to potentiate $Ca_V2.3$ channels. However in the elevation of $Ca_V2.3$ currents by M_1R activation, $PI(4,5)P_2$ seems more important factor than PKC because $PI(4,5)P_2$ hydrolysis produces DAG which recruits and activates PKC. When M_1R is activated by Oxo-M application, $Ca_V2.3$ currents are slightly decreased then gradually increased. That is the potentiating effect of PKC on $Ca_V2.3$ currents is stronger than the inhibitory effect of $PI(4,5)P_2$ depletion. Why is PKC effect on $Ca_V2.3$ channels stronger than other Ca_V2 family? That may be due to various potential phosphorylation sites in the α1 subunit of $Ca_V2.3$ channel. As mentioned in the introduction, $Ca_V2.3$ channels were potentiated by PKC activation. Actually, previous studies showed that both $Ca_V2.2$ and $Ca_V2.3$ currents were increased by PKC activation via application of PMA (40-41). Phosphorylation sites by PMA are embedded in I-II loop of α1 subunit (30-32). Except for I-II loop $Ca_V2.3$ channels have more phosphorylation sites than $Ca_V2.2$ channels in their II-III loop. Indeed, the sequence of II-III loop between $Ca_V2.3$ channels and $Ca_V2.1$ or $Ca_V2.2$ channels show much different (8). Therefore application of acetyl-β-methylcholine (MCh), another PKC activator, induced phosphorylation in II-III loop and further increase in $Ca_V2.3$ currents (31, 33).

Both Dr-VSP and PJ dephosphorylate $PI(4,5)P_2$ but inhibition ratio of PJ is higher than that of Dr-VSP (Figure 6, Figure 9, and Figure 10). The difference between Dr-VSP and PJ is that Dr-VSP transiently dephosphorylates $PI(4,5)P_2$ while PJ consistently dephosphorylates both PI(4)P and $PI(4,5)P_2$. PI(4)P is substrate of $PI(4,5)P_2$ so when $PI(4,5)P_2$ is depleted by Dr-VSP, $PI(4,5)P_2$ is rapidly replenished.

However since PJ dephosphorylates both PI(4)P and PI(4,5)P_2, current inhibition is strong.

According to our results, the inhibition ratio of $Ca_V2.2$ and $Ca_V2.3$ currents by the translocation of PJ was greater than that of INPP5E (Figure 9B and 10B) but the time constants of inhibition by INPP5E and PJ are similar (Figure 9C and 10C). This might be due to the rapid turnover between PI(4)P and PI(4,5)P_2 (38-39). In the plasma membrane, PI(4,5)P_2 was continuously and rapidly generated by phosphatidylinositol 4-phosphate 5-kinase from PI(4)P (38, 45). Since both INPP5E and PJ directly dephosphorylated PI(4,5)P_2, the time constants of inhibition in $Ca_V2.2$ or $Ca_V2.3$ current were similar (Figure 9C and 10C). However, INPP5E kept PI(4)P which is precursor of PI(4,5)P_2 intact and PI(4,5)P_2 was more rapidly synthesized and was replenished in the plasma membrane. Thus, the inhibition ratio of INPP5E seemed to be lower than that of PJ.

Also, we found that in cells expressing PJ-Sac with either $Ca_V2.2$ or $Ca_V2.3$ channels, the currents were decreased by translocation of PJ-Sac to the plasma membrane (Figure 9B and 10B). However, the time constants of currents inhibition by PJ-Sac were greater than when INPP5E or PJ were translocated (Figure 9C and 10C). As shown in the confocal experiments, we observed that four enzymes translocated to the plasma membrane immediately after application of rapamycin. We also observed that the increase in cytosolic PH-PLCδ-GFP intensity by PJ-Sac was lower than that of INPP5E or PJ (Figure 8C right), but the time constants by PJ-Sac was higher than that of INPP5E or PJ (Figure 8D right). These data indicated that the translocation of PJ-Sac was also able to induce PI(4,5)P_2 depletion. Here, we suggest that PJ-Sac dephosphorylates PI(4,5)P_2 via continuous turnover between PI(4)P and PI(4,5)P_2 for maintaining the equilibrium. In the plasma membrane, the amount of PI(4)P and PI(4,5)P_2 maintains almost 1:1 ratio by inositol polyphosphate 5-phosphatases such as oculocerebrorenal syndrome of Lowe 1 phosphatase (OCRL 1) (46). Altogether, PI(4,5)P_2 seems key factor regulating $Ca_V2.3$ currents.

Another regulator of HVA channels is $Ca_V\beta$ subunits. They regulate the physiological properties and expression level of HVA channels. They also regulate the channel sensitivity to PI(4,5)P_2, but, the sensitivity is different depending on the types of $Ca_V\beta$ subunits and their subcellular localization. For example, in cells expressing both $Ca_V2.2$ channels and Dr-VSP, currents with β3 subunits were

markedly decreased, but currents expressing β2a subunits showed little effect (47). Therefore, it is meaningful to test the effect of Ca_Vβ subunits on the regulation of Ca_V2.3 channels by $PI(4,5)P_2$ for better understanding the regulation mechanism of Ca_V2.3 channels.

In summary, our study is the first report showing the regulation of Ca_V2.3 channels by plasma membrane $PI(4,5)P_2$. Unlike previous studies, we revealed that Ca_V2.3 channels were inhibited by $PI(4,5)P_2$ depletion like other HVA channels (Figure 11). This study might contribute to extending our knowledge about regulation of Ca_V2.3 channels by phosphoinositide.

5. Figure legends

Figure 1. The role of voltage-gated calcium channels in calcium signaling

At resting state, concentration of calcium ions is higher in extracellular region. When depolarizing pulse activates VGCCs, extracellular calcium ions move to cytosol and calcium signaling begin.

Figure 2. Voltage-gated calcium channel (VGCC)

(A) Classification of VGCC. (B) The structure of VGCC. (C) Membrane topology of α1 subunit.

Figure 3. M_1R signaling pathway

M_1R signaling pathway is started when agonist binds to the receptor. Then $G_{q/11}$ protein is activated and the $G_{\alpha q}$ subunit activates phospholipase C (PLC). Activated PLCs hydrolyze PIP_2 into IP_3 and diacylglycerol (DAG). IP_3 increases the cytosolic Ca^{2+} level and DAG activates DAG activates PKC, respectively. PKCs phosphorylate their target protein such as ion channels, transcription factors, and scaffold proteins.

Figure 4. Differential modulation of $Ca_V2.2$ and $Ca_V2.3$ currents by M_1R activation

TsA201 cells were co-transfected with M_1 muscarinic receptor (M_1R) and either $Ca_V2.2$ or $Ca_V2.3$ channels. 10 μM of Oxotremorine-M (Oxo-M) was perfused for 60 s. (A) Left, time course of $Ca_V2.2$ currents. Right, Protocol generating $Ca_V2.2$ currents (*Upper*) and selected currents indicated in left graph (*Lower*). (B) Left, time course of $Ca_V2.3$ currents. Right, Protocol generating $Ca_V2.3$ currents (*Upper*) and selected currents indicated in left graph (*Lower*). (C) Summary graph of % inhibition by Oxo-M in $Ca_V2.2$ (n=13) and $Ca_V2.3$ (n=9) channels. Data are mean ± SEM.

Figure 5. Both $Ca_V2.2$ and $Ca_V2.3$ currents are suppressed by M_1R activation after full-activation of PKC

1 μM of phorbol 12-myristate 13-acetate (PMA) was applied for 2 min in tsA201 cells expressing M_1R and either $Ca_V2.2$ or $Ca_V2.3$ channels. Oxo-M was co-applied with PMA for 60 s. Normalized currents of (A) $Ca_V2.2$ channels (n=9) and (B) $Ca_V2.3$ channels (n=5). (C) Summary graph of % inhibition by Oxo-M of $Ca_V2.2$ (n=9) and $Ca_V2.3$ (n=5) currents. (D) The time constant for Oxo-M-induced inhibition of $Ca_V2.2$ (n=9) and $Ca_V2.3$ (n=5) currents. Data are mean ± SEM.

Figure 6. $PI(4,5)P_2$ depletion by Dr-VSP decreases both $Ca_V2.2$ and $Ca_V2.3$ currents

TsA201 cells were co-transfected with Dr-VSP and either $Ca_V2.2$ or $Ca_V2.3$ channels. (A) Standard protocol for measuring Dr-VSP activation of $Ca_V2.2$ and $Ca_V2.3$ currents. (B) Left, $Ca_V2.2$ currents in cells expressing Dr-VSP (n=9) or not (n=8). Right, $Ca_V2.3$ currents in the absence (n=6) or presence (n=5) of Dr-VSP. (C) Summary graph of % inhibition by depolarization in $Ca_V2.2$ currents. (D) Summary graph of % inhibition by depolarization in $Ca_V2.3$ currents. Data are mean ± SEM. *** P < 0.001, compared with - Dr-VSP.

Figure 7. Pseudojanin system

(A) $PI(4,5)P_2$ is dephosphorylated to PI(4)P by INPP5E. Sac1 dephosphorylates PI(4)P and produce PI (*upper*). Four translocatable enzymes (*lower*). (B) Principle of PJ system. Dimerization protein, FKBP and FRB for ternary complex with rapamycin and translocatable enzymes dephosphorylate their target molecules.

Figure 8. Plasma membrane PI(4,5)P_2 levels are reduced by translocation of PJ-Sac, INPP5E, and PJ

TsA201 cells were co-transfected with Lyn_{11}-FRB, PH-PLCδ-GFP, and one of the following four constructs; PJ-Dead, PJ-Sac, INPP5E, or PJ. (A) Confocal images of cells expressing PJ-Dead (upper left), PJ-Sac (upper right), INPP5E (lower left), or PJ (lower right) with PH-PLCδ-GFP. Images before (*Upper*) and after (*Lower*) the application of rapamycin (1 μM) for 180 s (Scale bar, 5 μm). (B) Time courses of cytosolic PH-PLCδ-GFP, and translocatable enzymes intensity in cells expressing PJ-Dead (upper left), PJ-Sac (upper right), INPP5E (lower left), or PJ (lower right). (C) Summary graph of % decrease in the intensity of translocatable enzymes (left) and % increase in the intensity of PH-PLCδ-GFP (right) (D) Time constant of decrease in translocatable enzyme intensity (left) and time constant of increase in PH-PLCδ-GFP intensity by addition of rapamycin (n=4 for PJ-Dead; n=7 for PJ-Sac; n=8 for INPP5E; and n=9 for PJ).

Figure 9. $Ca_V2.2$ currents were suppressed by depletion of PI(4)P, PI(4,5)P_2, and both PI(4)P and PI(4,5)P_2

TsA201 cells were co-transfected with $Ca_V2.2$ channels, Lyn_{11}-FRB (plasma membrane anchoring protein), and one of the four constructs; PJ-Dead, PJ-Sac, INPP5E, or PJ. Rapamycin was applied for 60 s. (A) Time courses of $Ca_V2.2$ currents in cells expressing PJ-Dead, PJ-Sac, INPP5E, or PJ. (B) Summary graph of % inhibition by rapamycin addition in $Ca_V2.2$ currents (n=6 for PJ-Dead; n=9 for PJ-Sac; n=5 for INPP5E; and n=11 for PJ). (C) Summary graph of the time constant for rapamycin-induced inhibition in $Ca_V2.2$ currents (n=9 for PJ-Sac; n=5 for INPP5E; and n=11 for PJ). Data are mean ± SEM. **P* < 0.05, ***P* < 0.01, and ****P* < 0.001, with one-way ANOVA followed by Bonferroni post-hoc test.

Figure 10. $Ca_V2.3$ currents were suppressed by depletion of PI(4)P, PI(4,5)P_2, and both PI(4)P and PI(4,5)P_2

$Ca_V2.3$ channels were expressed in tsA201 cells with Lyn_{11}-FRB and one of the four constructs; PJ-Dead, PJ-Sac, INPP5E, or PJ. Rapamycin was added for 60 s. (A) Time courses of $Ca_V2.3$ currents in

cells expressing PJ-Dead, PJ-Sac, INPP5E, or PJ. (B) Summary of % inhibition by rapamycin in $Ca_V2.3$ currents (n=3 for PJ-Dead; n=5 for PJ-Sac; n=6 for INPP5E; and n=7 for PJ). (C) Summary graph of the time constant for rapamycin-induced inhibition in $Ca_V2.3$ currents (n=5 for PJ-Sac; n=6 for INPP5E; and n=7 for PJ). Data are mean ± SEM. *P < 0.05, **P < 0.01, and ***P < 0.001, with one-way ANOVA followed by Bonferroni post-hoc test.

Figure 11. Modulation of $Ca_V2.3$ channel by M_1R

$PI(4,5)P_2$ depletion by M_1R activation inhibits $Ca_V2.3$ channel. However, since the potentiation by PKC is stronger than the suppression by $PI(4,5)P_2$ depletion, $Ca_V2.3$ channels is opened and induce Ca^{2+} influx.

6. Figures

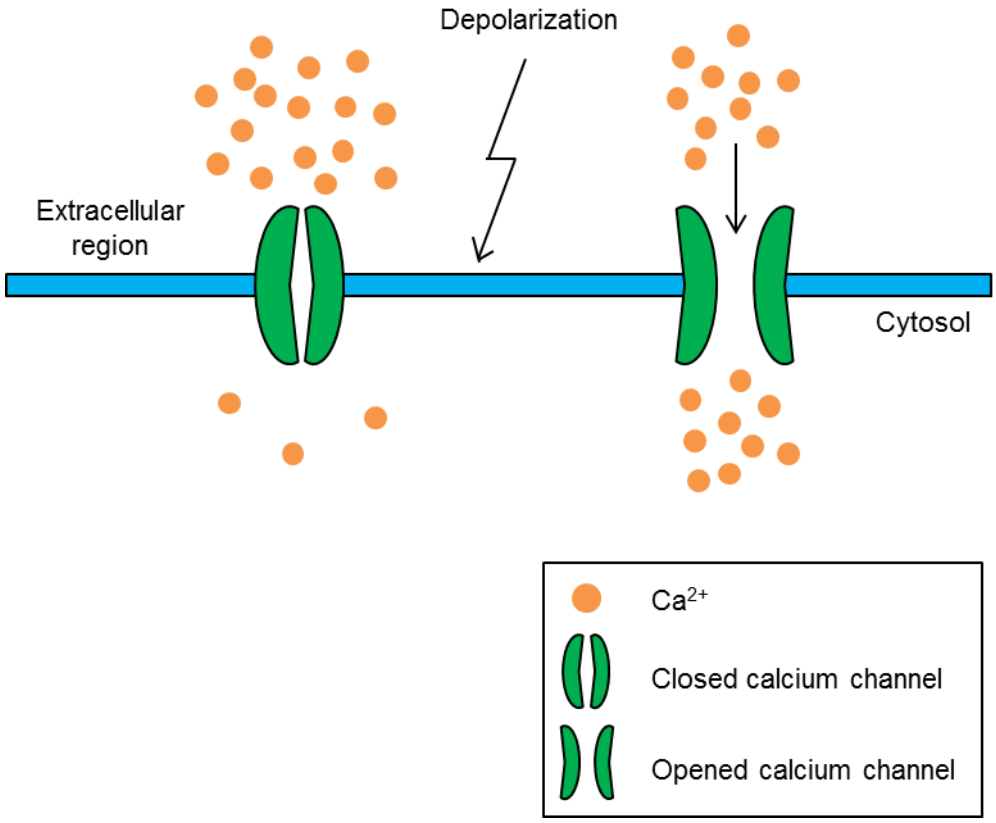

Figure 1. The role of voltage-gated calcium channels in calcium signaling

A

HVA	L-type		$Ca_V1.1$ (α1F)
			$Ca_V1.2$ (α1C)
			$Ca_V1.3$ (α1D)
			$Ca_V1.4$ (α1S)
	Neuronal type	P/Q-type	$Ca_V2.1$ (α1A)
		N-type	$Ca_V2.2$ (α1B)
		R-type	$Ca_V2.3$ (α1E)
LVA	T-type		$Ca_V3.1$ (α1G)
			$Ca_V3.2$ (α1H)
			$Ca_V3.3$ (α1I)

B

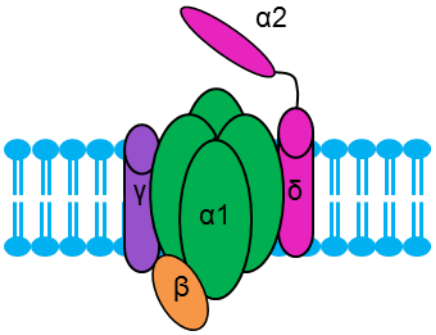

C

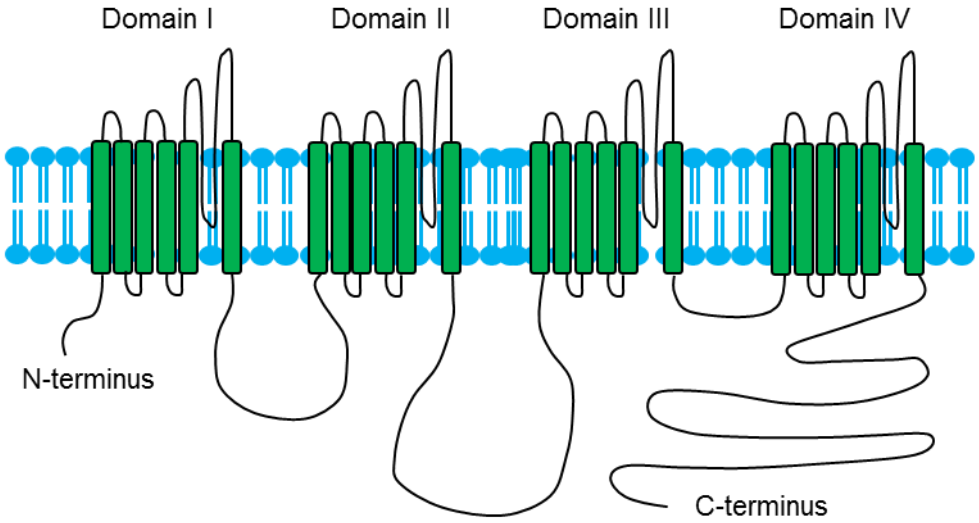

Figure 2. Voltage-gated calcium channel (VGCC)

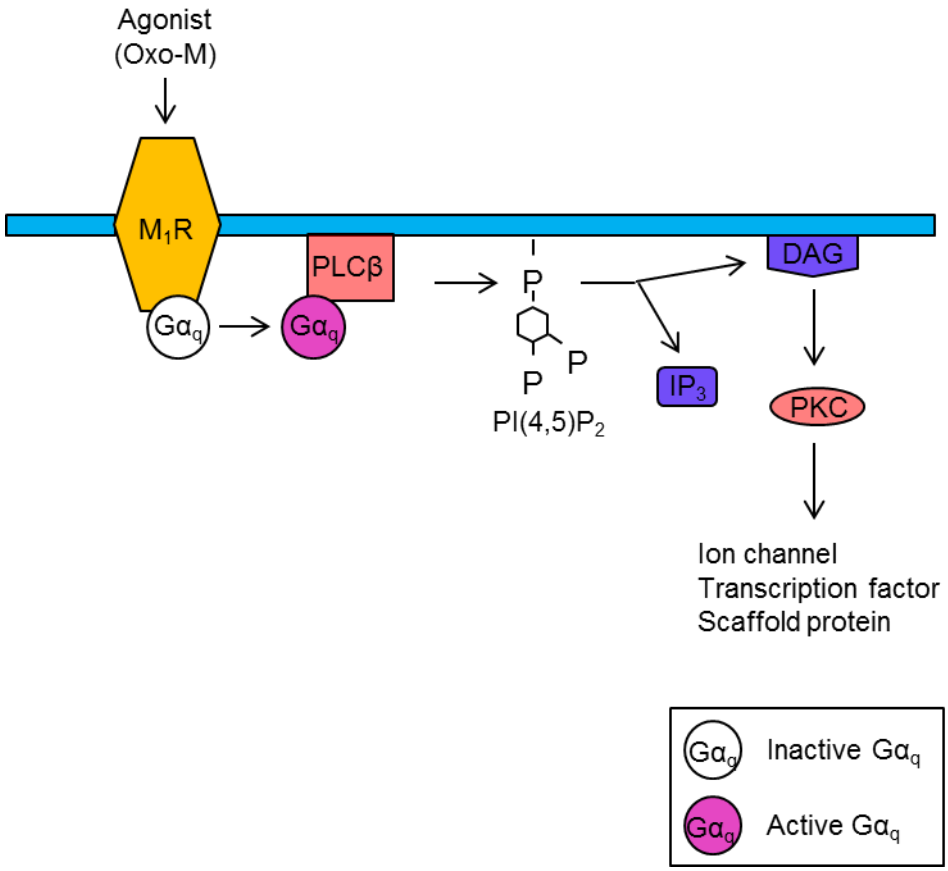

Figure 3. M_1R signaling pathway

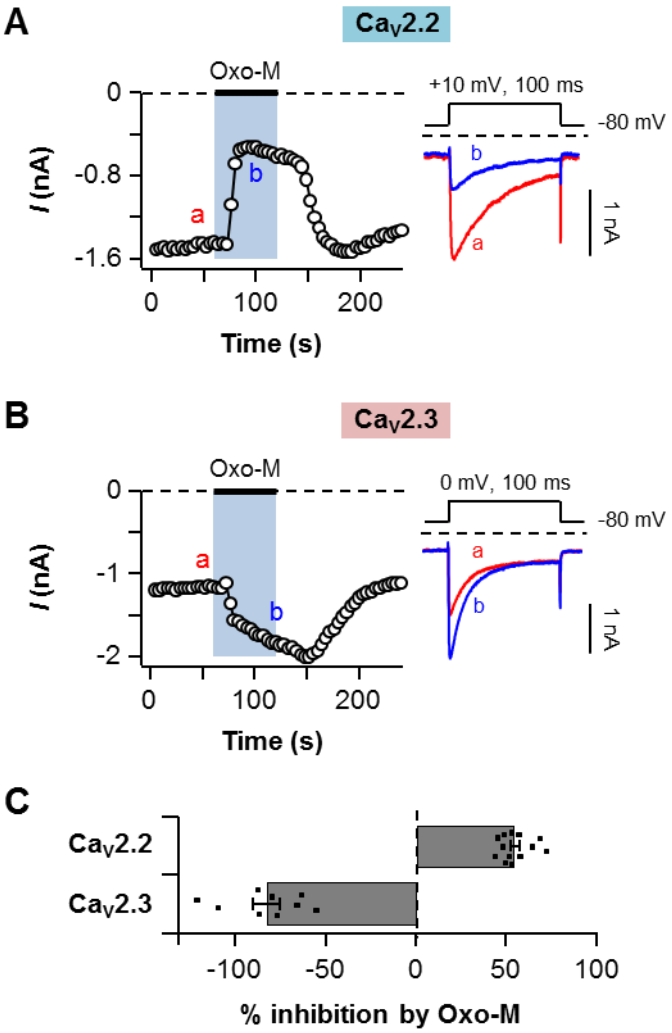

Figure 4. Differential modulation of $Ca_V2.2$ and $Ca_V2.3$ currents by M_1R activation

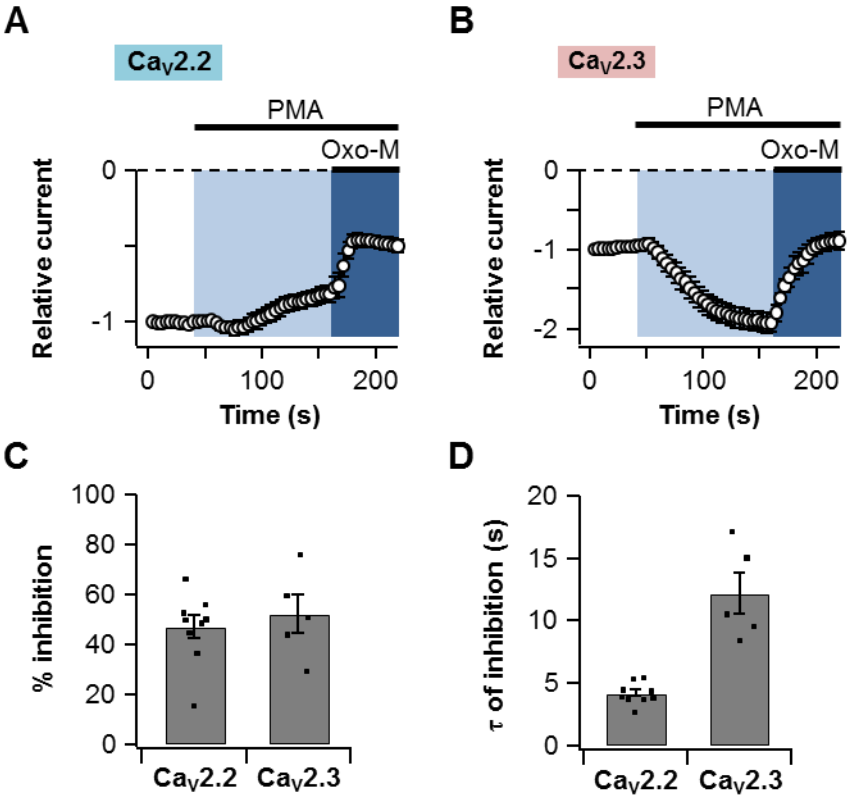

Figure 5. Both $Ca_V2.2$ and $Ca_V2.3$ currents are suppressed by M_1R activation after full-activation of PKC

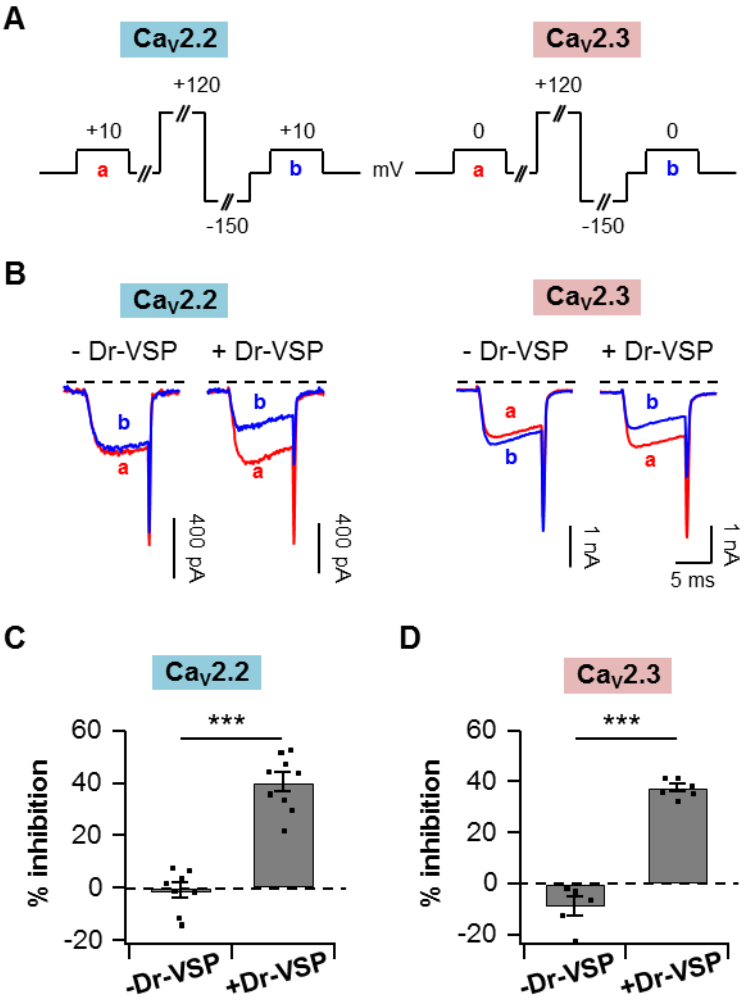

Figure 6. PI(4,5)P_2 depletion by Dr-VSP decreases both $Ca_V2.2$ and $Ca_V2.3$ currents

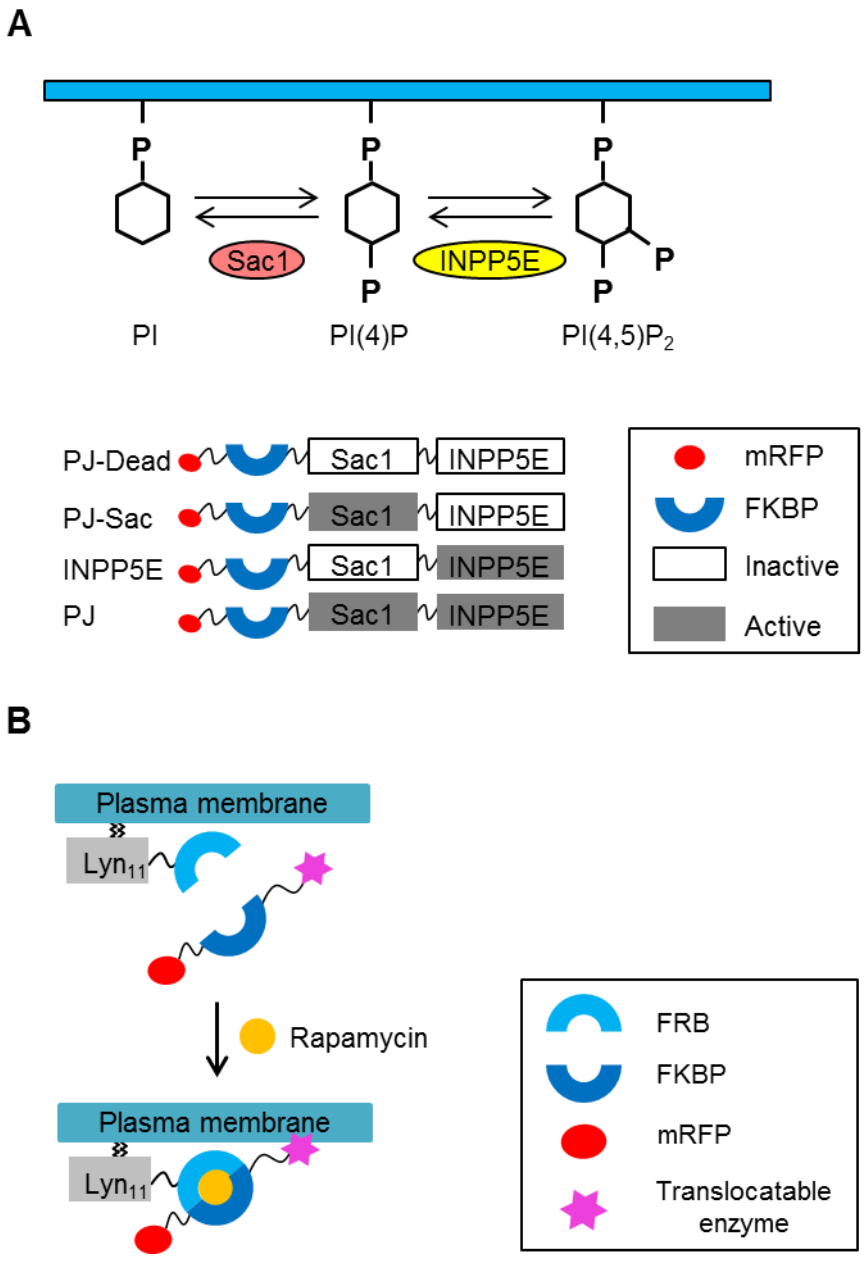

Figure 7. Pseudojanin-system

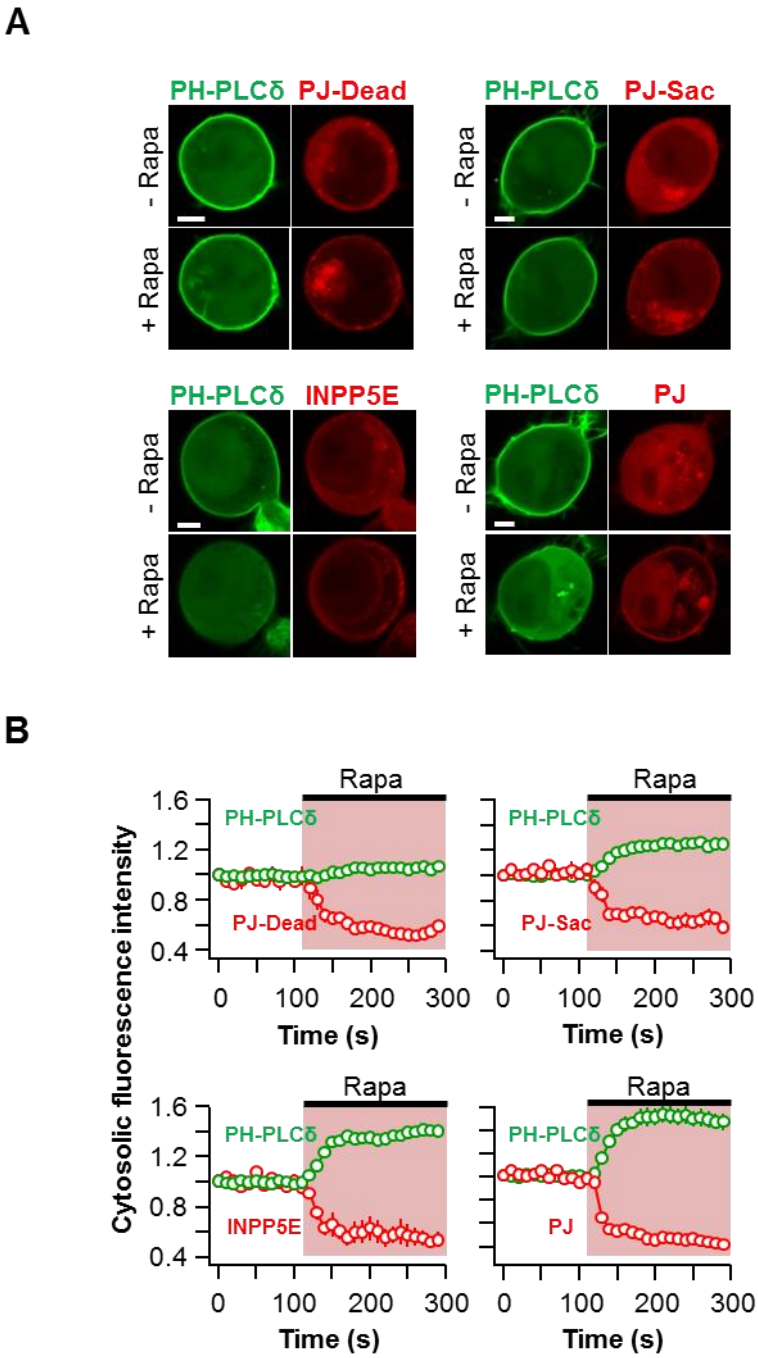
A
PH-PLCδ PJ-Dead
PH-PLCδ PJ-Sac
PH-PLCδ INPP5E
PH-PLCδ PJ
- Rapa
+ Rapa
B
Rapa
PH-PLCδ
PJ-Dead
PJ-Sac
INPP5E
PJ
Cytosolic fluorescence intensity
1.6
1.2
0.8
0.4
0
100
200
300
Time (s)

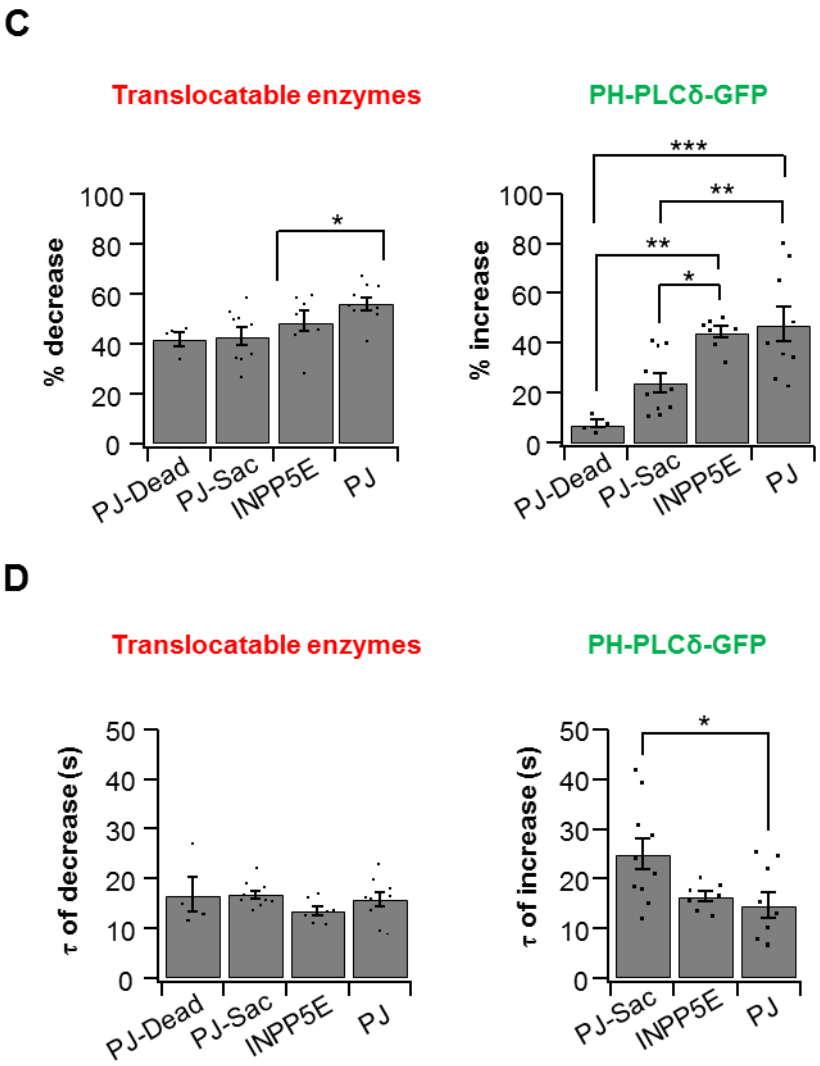

Figure 8. Plasma membrane PI(4,5)P_2 levels are reduced by translocation of PJ-Sac, INPP5E, and PJ

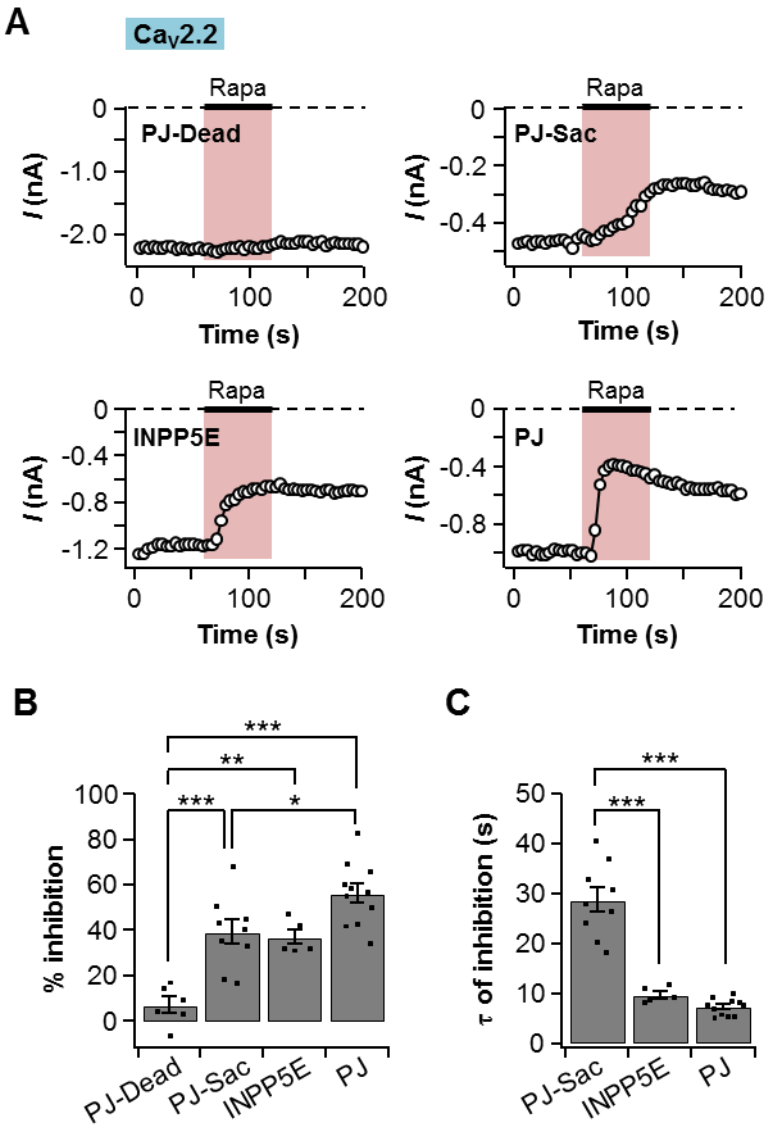

Figure 9. $Ca_V2.2$ currents were suppressed by depletion of PI(4)P, $PI(4,5)P_2$, and both PI(4)P and $PI(4,5)P_2$

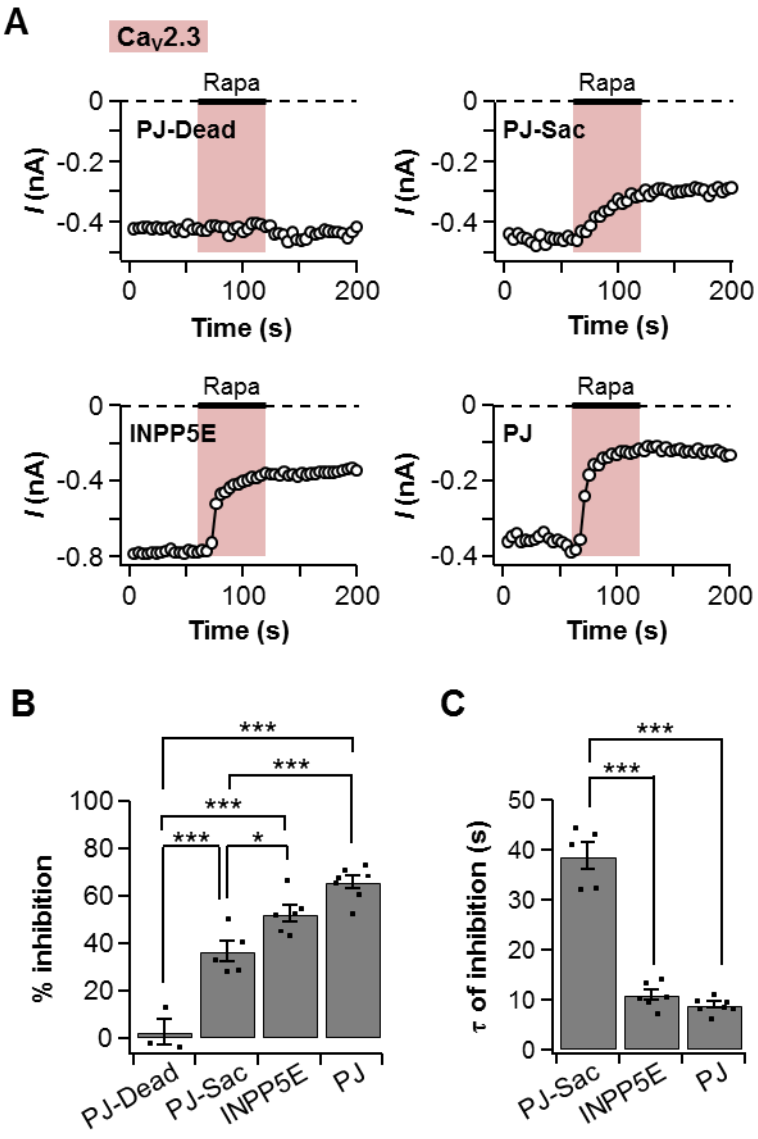

Figure 10. $Ca_V2.3$ currents were suppressed by depletion of PI(4)P, $PI(4,5)P_2$, and both PI(4)P and $PI(4,5)P_2$

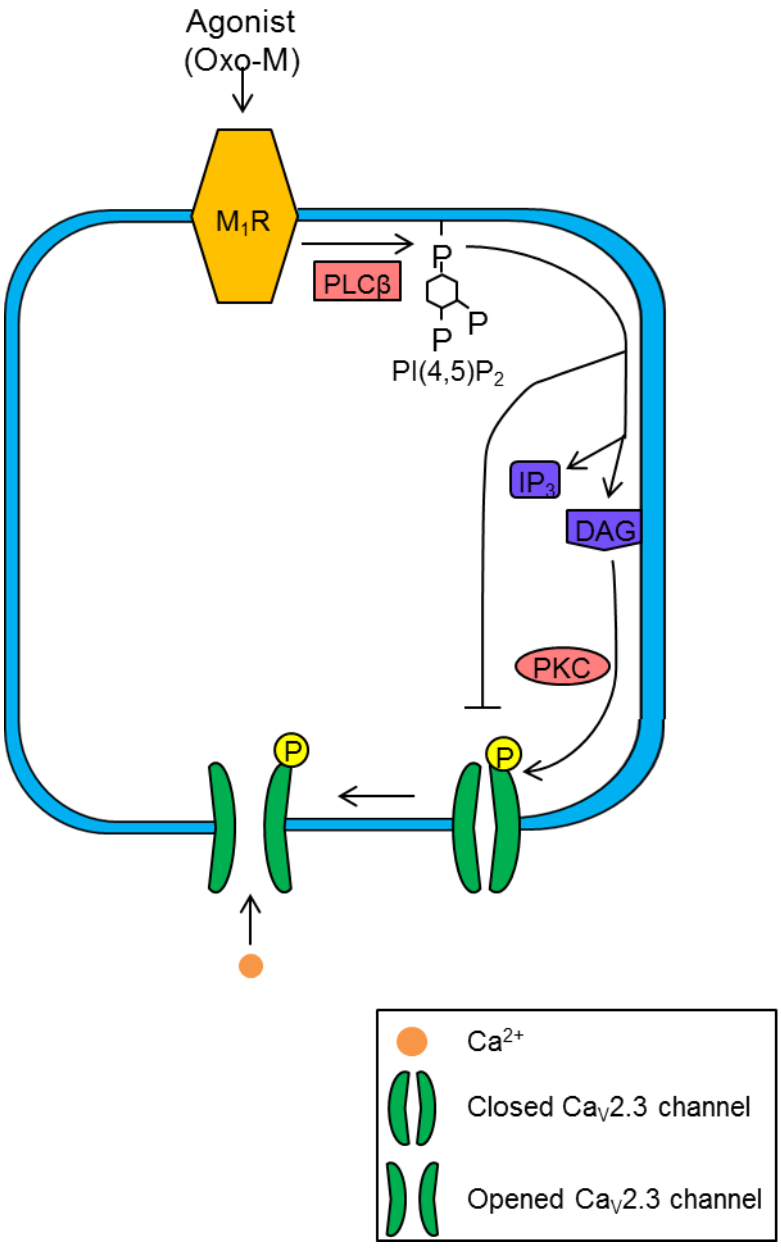

Figure 11. Modulation of $Ca_V2.3$ channel by M_1R

References

1. Simms BA, and Zamponi GW (2014). “Neuronal Voltage-Gated Calcium Channels: Structure, Function, and Dysfunction.” *Neuron*, 82(1), pp. 24-45.

2. Berridge MJ (2012). “Cell Signalling Pathways.” Biochemical J

3. Catterall WA, Perez-Reyes E, Snutch TP, and Striessnig J. (2005). “International Union of Pharmacology. XLVIII. Nomenclature and Structure-Function Relationships of Voltage-Gated Calcium Channels.” *Pharmacol Rev*, 57(4), pp. 411-25.

4. Lacinoa L. (2005). “Voltage-dependent Calcium Channels.” *Ph.D. Thesis*, Institute of Molecular Physiology and Genetics Slovak Academy of Sciences, Vlarska 5, 833 34 Bratislava 37, Slovakia, 78 pages.

5. Niidome T, Kim MS, Friedrich T, and Mori Y. (1992). “Molecular cloning and characterization of a novel calcium channel from rabbit brain.” *FEBS Lett*, 308(1), pp. 7-13.

6. Soong TW, Stea A, Hodson CD, Dubel SJ, Vincent SR, and Snutch TP. (1993). “Structure and functional expression of a member of the low voltage-activated calcium channel family.” *Science*, 260(5111), pp. 1133-6.

7. Williams ME, Marubio LM, Deal CR, Hans M, Brust PF, Philipson LH, Miller RJ, Johnson EC, Harpold MM, and Ellis SB. (1994). “Structure and functional characterization of neuronal α1E channel subtypes.” *J Biol Chem*, 269(35), pp.22347-57.

8. Wu LG, Borst JG, and Sakmann B. (1998). “R-type Ca^{2+} currents evoke transmitter release at a rat central synapse.” *Proc Natl Acad Sci USA*, 95(8), pp. 4720-5.

9. Saequsa H, Kurihara T, Zong S, Minowa O, Kazuno A, Han W, Matsuda Y, Yamanaka H, Osanai M, Noda T, and Tanabe T. (2000). “Altered pain responses in mice lacking α1E subunit of the voltage-dependent Ca^{2+} channel.” *Proc Natl Acad Sci USA*, 97(11), pp. 6132-7.

10. Lee SC, Choi S, Lee T, Kim HL, Chin H, and Shin HS. (2002). “Molecular basis of R-type calcium channels in central amygdala neurons of the mouse.” *Proc Natl Acad Sci USA*, 99(5), pp. 3276-81.

11. Ishii M, and Kurachi Y. (2006). “Muscarinic Acetylcholine Receptors.” *Curr Pharm Des*, 12(28), pp. 3573-81.

12. Thiele A (2013). “Muscarinic Signaling in the Brain.” *Annu Rev Neurosci*, 36, pp. 271-94.

13. Melliti K, Meza U, and Adams B. (2000). “Muscarinic stimulation of α1E Ca channels is selectively blocked by the effector antagonist function of RGS2 and phospholipase C-β1.” *J neurosci*, 20(19), pp. 7167-73.

14. Bannister RA, Melliti K, and Adams BA. (2004). “Differential modulation of $Ca_V2.3$ Ca^{2+} channels by $G\alpha_{q/11}$-coupled muscarinic receptors.” *Mol Pharmacol*, 65(2), pp. 381-8.

15. Tai C, Kuzmiski, and MacVicar BA. (2006). “Muscarinic enhancement of R-type calcium currents in hippocampal CA1 pyramidal neurons.” *J Neurosci*, 26(23), pp. 6249-58.

16. Shapiro MS, Loose MD, Hamilton SE, Nathanson NM, Gomeza J, Wess J, and Gille B.

(1999). “Assignment of muscarinic receptor subtypes mediating G-protein modulation of Ca^{2+} channels by using knockout mice.” *Proc Natl Acad Sci USA*, 96(19), pp. 10899-904.

17. Kammermeier PJ, Ruiz-Velasco V, and Ikeda SR. (2000). “A voltage-independent calcium current inhibitory pathway activated by muscarinic agonists in rat sympathetic neurons requires both $G\alpha_{q/11}$ and $G\beta\gamma$.” *J Neurosci*, 20(15), pp. 5623-9.

18. Melliti K, Meza U, and Adams BA. (2001). “RGS2 blocks slow muscarinic inhibition of N-type Ca^{2+} channels reconstituted in a human cell line.” *J Physiol*, 532(Pt 2), pp. 337-47.

19. Gamper N, Reznikov V, Yamada Y, Yang J, and Shapiro MS. (2004). “Phosphatidylinositol 4,5-bisphosphate signals underlie receptor-specific $G_{q/11}$-mediated modulation of N-type Ca^{2+} channels.” *J Neurosci*, 24(48), pp. 10980-92.

20. Perez-Burgos A, Perez-Rosello T, Salgado H, Flores-Barrera E, Prieto GA, Fugueroa A, Galarraga E, and Bargas J. (2008). “Muscarinic M_1 modulation of N and L types of calcium channels is mediated by protein kinase C in neostriatal neurons.” *Neuroscience*, 155(4), pp. 1079-97.

21. Perez-Burgos A, Prieto GA, Galarraga E, and Bargas J. (2010). “$Ca_V2.1$ channels are modulated by muscarinic M_1 receptors through phosphoinositied hydrolysis in neostriatal neurons.” *Neuroscience*, 165(2), pp. 293-9.

22. Prescott ED, and Julius D. (2003). “A modular PIP_2 binding site as a determinant of capsaicin receptor sensitivity.” *Science*, 300(5623), pp. 1284-8.

23. Hilgemann DW. (2007). “On the physiological roles of PIP_2 at cardiac Na^+-Ca^{2+} exchangers and K_{ATP} channels: a long journey from membrane biophysics into cell biology.” *J Physiol*, 582(Pt 3), pp. 903-9.

24. Pochynyuk O, Medina J, Gamper N, Genth H, Stockand JD, and Staruschenko A. (2006) “Rapid translocation and insertion of the epithelial Na^+ channel in response to RhoA signaling.” *J Biol Chem*, 281(36), pp.26520-7.

25. Koriyama N, Kakei M, Nakazaki M, Yaekura K, Ichinari K, Gong Q, Morimitsu S, Yada T, and Tei C. (2000) “PIP_2 and ATP cooperatively prevent cytosolic Ca^{2+}-induced modification of ATP-sensitive K^+ channels in rat pancreatic β-cells.” *Diabetes*, 49(11), pp. 1830-9.

26. Liang H, DeMaria CD, Erickson MG, Mori MX, Alseikhan BA, and Yue DT. (2003). “Unified mechanisms of Ca^{2+} regulation across the Ca^{2+} channel family.” *Neuron*, 39(6), pp. 951-960. 23

27. Suh BC, Leal K, and Hille B. (2010). “Modulation of high-voltage activated Ca^{2+} channels by membrane phosphatidylinositol 4,5-bisphosphate.” *Neuron*, 67(2), pp. 224-38.

28. Perez-Rosello T, Figueroa A, Salgado H, Vilchis C, Tecuapetia F, Guzman JN, Galarraga E, and Bargas J. (2004). “Cholinergic control of firing pattern and neurotransmission in rat neostriatal projection neurons: role of $Ca_V2.1$ and $Ca_V2.2$ Ca^{2+} channels.” *J Neurophysiol*, 93(5), pp. 2507-19.

29. Stea A, Soong TW, and Snutch TP. (1995). “Determinants of PKC-dependent modulation of a family of neuronal calcium channels.” *Neuron*, 15(4), pp. 929-40.

30. Kamatchi GL, Tiwari SN, Chan CK, Chen D, Do SH, Durieux ME, and Lynch C 3rd. (2003). “Distinct regulation of expressed calcium channels 2.3 in Xenopus oocytes by direct or indirect activation of protein kinase C.” *Brain Res*, 968(2), pp. 227-37.

31. Kamatchi GL, Franke R, Lynch C 3rd, and Sando JJ. (2004). “Identification of sites

responsible for potentiation of type 2.3 calcium currents by acetyl-β-methylcholine." *J Biol Chem*, 279(6), pp. 4102-9.

32. Fang H, Franke R, Patanavanich S, Lalvani A, Powell NK, Sando JJ, and Kamatchi GL. (2005). "Role of α1 2.3 subunit Ⅰ-Ⅱ linker sites in the enhancement of $Ca_V2.3$ current by phorbol 12-myristate 13-acetate and acetyl-β-methylcholine." *J Biol Chem*, 208(25), pp. 23559-65.

33. Rajagopal S, Fang H, Patanavanich S, Sando JJ, and Kamatchi GL. (2008). "Protein kinase C isozyme-specific potentiation of expressed $Ca_V2.3$ currents by acetyl-β-methylcholine and phorbol-12-myristate, 13-acetate." *Brain Res*, 1210, pp. 1-10.

34. Hammond GR, Fischer MJ, Anderson KE, Holdich J, Koteci A, Balla T. and Irvine RF. (2012). "PI4P and $PI(4,5)P_2$ are essential but independent lipid determinants of membrane identity." *Science*, 337(6095), pp. 727-30.

35. Guo S, Stolz LE, Lemrow SM, and York JD (1999). "SAC1-like domains of yeast SAC1, INP52, and INP53 and of human synaptojanin encode polyphosphoinositide phosphatases." *J Biol Chem*, 274(19), pp. 12990-5.

36. Bielas SL, Silhavy JL, Brancati F, Kisseleva MV, Al-Gazali L, Sztriha L, Bayoumi RA, Zaki MS, Abdel-Aleem A, Rosti RO, Kayserili H, Swistun D, Scott LC, Bertini E, Boltshauser E, Fazzi E, Travaglini L, Field SJ, Gayral Sm Jacoby M, Schurmans S, Dallapiccola B, Majerus PW, Valente EM, and Gleeson JG (2009). "Mutations in INPP5E, encoding inositol polyphosphate-5-phosphatase E, link phosphatidyl inositol signaling to the ciliopathies." *Nat Genet*, 41(9), pp. 1032-6.

37. Inoue T, Heo WD, Grimley JS, Wandless TJ, and Meyer T. (2005). "An inducible translocation strategy to rapidly activate and inhibit small GTPase signaling pathways." *Nat Methods*, 2(6), pp. 415-8.

38. Wuttke A, Sågetorp J and Tengholm A. (2010). "Distinct plasma-membrane PtdIns(4)P and $PtdIns(4,5)P_2$ dynamics in secretagogue-stimulated β–cells." J Cell Sci, 123(Pt9), pp. 1492-502.

39. Oude Weernink, Schmidt M, and Jakobs KH. (2004). "Regulation and cellular roles of phosphoinositide 5-kinases." Eur J Pharmacol, 500(1~3), pp. 87-99.

40. Suh BC, and Hille B. (2008). "PIP_2 is a necessary cofactor for ion channel function: How and why?" Annu Rev Biophys, 37, pp. 175-95.

41. Rohacs T. (2009). "Phosphoinositide regulation of non-canonical transient receptor potential channels." Cell Calcium, 45(6), pp. 554-65.

42. Hilgemann DW, Feng S, and Nasuhoglu C. (2001). "The complex and intriguing lives of PIP_2 with ion channels and transporters." *Sci STKE*, 2001(111), pp, re19.

43. Zamponi GW, Bourinet E, Nelson D, Nargeot J, and Snutch TP. (1997). "Crosstalk between G proteins and protein kinase C mediated by the calcium channel α1 subunit." *Nature*, 385(6615), pp. 442-6.

44. Hamid J, Nelson D, Spaetgens R, Dubel SJ, Snutch TP, and Zamponi GW. (1999). "Identification of an integration center for cross-talk between protein kinase C and G protein modulation of N-type calcium channels." *J Biol Chem*, 274(10), pp. 6195-202.

45. Balla T. (2013). "Phosphoinositides: tiny lipids with giant impact on cell regulation." *Physiol Rev*, 93(3), pp. 1019-137.

46. Kwiatkowska K. (2010). “One lipid, multiple functions: how various pools of $PI(4,5)P_2$ are created in the plasma membrane.” *Cell Mol Life Sci*, 67(23), pp. 3927-46.

47. Suh BC, Kim DI, Falkenburger BH, and Helle B. (2012) “Membrane-localized β-subunits alter the PIP_2 regulation of high-voltage activated Ca^{2+} channels.” Proc Natl Acad Sci USA, 109(8), pp. 3161-6.

요약문

많은 전압 개폐 칼슘 채널은 G_q 단백질 연결 수용체 (G_q-protein coupled receptor, G_qPCR) 중 하나인 무스카린성 아세틸콜린 수용체에 의해서 조절된다. 전압 개폐 칼슘 채널 중 $Ca_V2.3$ 채널의 전류는 M_1 무스카린성 수용체에 의해서 증가하며 이 때 전류의 증가는 단백질 인산화 효소 C에 의한 채널의 인산화 때문이라고 알려져 있다. 실제로 $Ca_V2.3$ 채널을 발현하는 tsA201 세포에 phorbol 12-myristate 13-acetate (PMA) 라는 단백질 인산화 효소 C의 활성제를 처리할 경우 $Ca_V2.3$ 채널의 전류가 두 배 가량 증가하는 것을 보았다. 흥미로운 점은 PMA 를 처리해서 $Ca_V2.3$ 채널을 완전히 활성화 시킨 후 M_1 수용체를 활성화 시키면 $Ca_V2.3$ 채널의 전류가 줄어든다는 점이다. 우리는 전류를 억제시키는 요인을 찾기 위해서 M_1 수용체에 의해 일어나는 신호전달계를 살펴보았다. M_1 수용체가 활성화 되면 세포막에 있는 $PI(4,5)P_2$ 라는 인지질이 분해된다. $Ca_V2.3$ 채널과 같은 그룹인 $Ca_V2.2$ 채널이 $PI(4,5)P_2$ 양이 감소하면 전류가 줄어든다는 보고가 있기 때문에 $PI(4,5)P_2$ 가 $Ca_V2.3$ 채널의 억제에도 영향을 미치는지 알아보기로 했다. 첫 번째로 높은 전압 (+120 mV)을 가해줬을 때 활성화되는 인산 가수분해 효소를 이용했다. 우리는 이 방법을 통해서 $Ca_V2.3$ 채널의 전류가 38% 가량 줄어든다는 것을 알아냈다. 두 번째로 특정 화학물질을 첨가하였을 때 두 개의 분자가 이합체화 되는 현상을 이용하는 방법을 사용했다. 이 방법을 이용해서 인산 가수분해 효소를 세포막으로 가져올 수 있고 인지질을 분해 할 수 있다. 우리는 라파마이신이라는 화학물질을 이용해서 인산 가수분해 효소를 세포막으로 이동시킨 후 $PI(4,5)P_2$의 양을 감소시켰다. 그 결과 $Ca_V2.3$ 채널의 전류가 66% 정도 줄어드는 것을 발견했다. 위의 실험결과들은 $Ca_V2.3$ 채널의 전류가 M_1 수용체에 의해서 활성화 될 수도 있고 억제될 수도 있다는 것을 보여준다. 활성화되는 기작은 단백질 인산화 효소 C에의한 $Ca_V2.3$ 채널의 인산화 때문이고 억제되는 기전은 세포막에 있는 $PI(4,5)P_2$ 의 감소에 의한 것이다. 이 연구를 통해서 세포막에 있는 $PI(4,5)P_2$는 $Ca_V2.3$ 채널의 활성을 유지하고 조절하는데 중요한 역할을 한다는 것을 밝혀냈다.